JOURNAL OF MATERIALS SCIENCE 10 (1975) 399–405

# SEM investigations of iron surface ion erosion as a function of specimen temperature and incidence angle

F. VASILIU,* I. A. TEODORESCU†
*Institute of Atomic Physics, P.O. Box 35, Bucharest, Romania*

F. GLODEANU
*Institute of Nuclear Technology, P.O. Box 4615, Bucharest, Romania*

Ion bombardment of iron surfaces produced an ion eroded surface microtopography strongly dependent on the incidence angle and specimen temperature. For bombardment temperatures exceeding the self-diffusion temperature, $T_d$, a microstructural smoothing process due to the thermally activated diffusion effects, assisted by ion bombardment, can be observed by SEM. The role of migrational processes which should be taken into account for a correct interpretation of the final surface topography formed by "hot sputtering", was also considered.

## 1. Introduction

In recent years, there has been an increase in the amount of data, and an improvement in the relevant theory concerning surface microtopography induced by ion bombardment. Arising from this, a clearer picture of this phenomenon and possible explanations have been built up.

The dependence of surface microtopography on the incidence angle of the ion beam was pointed out by many authors [1-4] and, on the basis of experimental and theoretical results accumulated to date, it is assumed that this is a general phenomenon for all crystalline and amorphous materials. Experimentally, the surface ion erosion effects can be characterized by "scale-shaped" microreliefs, etch lines, cones, furrows, hillocks, etc., which are all approximately parallel and opposite to the tangential component of the ion beam.

In recent theoretical works, the development of some topographical features has been successfully explained and predicted using Franks' kinematic theory of crystal dissolution [5] or erosion slowness curves which define the directions and the velocities of points of constant orientation on the sputtered surface [6]. Both treatments describe the occurrence of regular ion erosion surface features as a result of a non-monotonic dependence of sputtering rate upon angle of incidence to each point on the surface. Reduction or increase in local sputtering rate can result from the location of the deposited-energy function maximum at a finite distance from the point of ion impact, which results in an enhancement of small irregularities during ion bombardment [7].

Some significant deviations of the ion microrelief from these recent theoretical predictions can be expected as a result of the following simultaneous secondary processes: (1) the redeposition of sputtered material on to closely adjacent planes; (2) the ion reflection at grazing incidence [8]; (3) dechannelling at dislocation lines [9]; (4) the surface binding energy modifications arising from variations in crystallographic orientation or elastic stress [10]; (5) diffusion processes.

Although there is total agreement concerning the important role played by sample temperature on the ion sputtered microrelief, the surface smoothing due to the diffusion effects which act together with sputtering during ion bombardment at elevated temperatures, has usually not been taken into consideration in the various mechanisms proposed for nucleation and growth

*Present address: Institut für Material- und Festkörperforschung, KFK, P.O. Box 3640, Karlsruhe, W. Germany.
†Present address: IAEA, P.O. Box 645, Vienna, Austria.

of radiation-induced microtopography [6, 7, 11]. In addition, until now little data on the evolution of sputter-topographies with increasing temperature for heated metallic targets subjected to ion bombardment have been available [3, 12, 13].

The present investigation aimed to show the complex role played by the sample temperature and ion incidence angle on the final ion-eroded microtopography developed on polycrystalline iron and studied by SEM.

## 2. Experimental

The iron samples were bombarded with argon ion beams of energy of 20 keV and density 300 $\mu A\ cm^{-2}\ sec^{-1}$ at incidence angles of $\phi = 0°$, 30°, 45° and 60°. The specimen temperature was varied between 20 and 900°C with a constant irradiation time (30 min) and vacuum ($p \leqslant 5 \times 10^{-5}$ Torr) during bombardment. The specimen heater was mounted in a goniometric facility so that the beam direction could be adjusted and reproduced easily.

The microtopography of the irradiated targets was investigated using a JSM-4C scanning electron microscope. The viewing angle was 45° with respect to the surface normal, for all SEM micrographs.

## 3. Results and discussion

Ion bombardment of iron surfaces, which initially had a regular microtopography formed by thermal etching and characterized by pyramid-shaped growths at the points where the dislocations intersect the surface [14], produced an ion eroded microrelief, strongly dependent on the incidence angle and the initial microrelief, showing various local inclinations to the parallel ion beam [4]. The typical ion etching patterns (etch lines and "scale-shaped" microreliefs), occurring for inclined incidence angles on various crystalline solids (metals, semiconductors, ceramics, alkali halides) or amorphous materials (glass, glass-ceramics) can be explained on the basis of two factors: (a) the surface microgeometry existing before ion bombardment; (b) the angular dependence of the sputtering yield $S = S(\phi)$.

The combined effect of the bombardment temperature ($20°C \leqslant t \leqslant 900°C$) and incidence angle ($\phi = 0°$, 30° 45°, 60°) on iron surface sputtered topography has been investigated by SEM in the present work. The aspects revealed for ion bombardment at room temperature given in [4] are not discussed here.

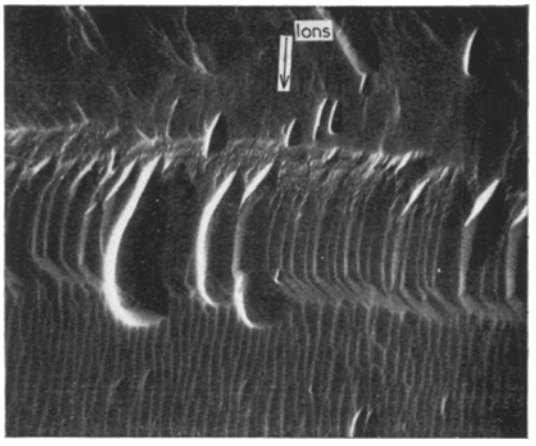


*Figure 1* Iron surface, bombarded with 20 keV $Ar^+$ ions at $\phi = 30°$ for 30 min ($t = 300°C$) × 3000.

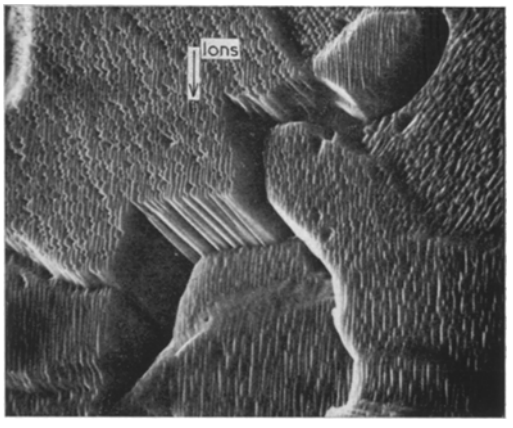


*Figure 2* Iron surface, bombarded with 20 keV $Ar^+$ ions at $\phi = 45°$ for 30 min ($t = 300°C$) × 3000.

Some microstructural aspects, typical for ion erosion at $t = 300°C$, $\phi = 30°$ and 45° respectively, are illustrated in Figs. 1 and 2, where "scale-shaped" figures and etch lines may be seen to invariably point in the opposite direction to the incident ion beam; this is also characteristic for room temperature bombardment. An additional weak effect of thermal facetting can be easily observed in Fig. 2 even at this temperature. At $\phi = 60°$, the etch lines become predominant, being parallel to the ion beam on all grains.

At $t = 400°C$, $\phi = 45°$ (Fig. 3) the thermal facetting induces an undulatory substructure of etch lines which have a major component along the ion beam direction. Microstructures revealed

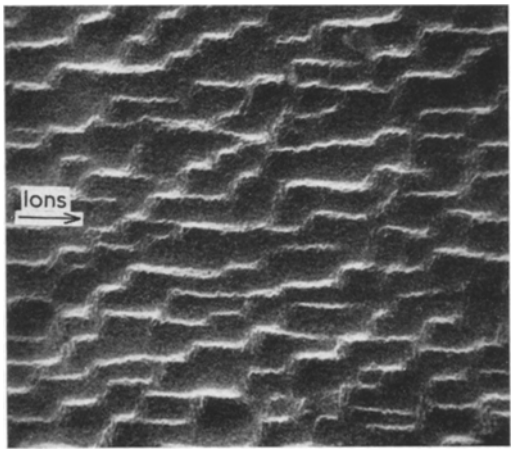


*Figure 3* Iron surface, bombarded with 20 keV $Ar^+$ ions at $\phi = 45°$ for 30 min ($t = 400°C$) × 6000.

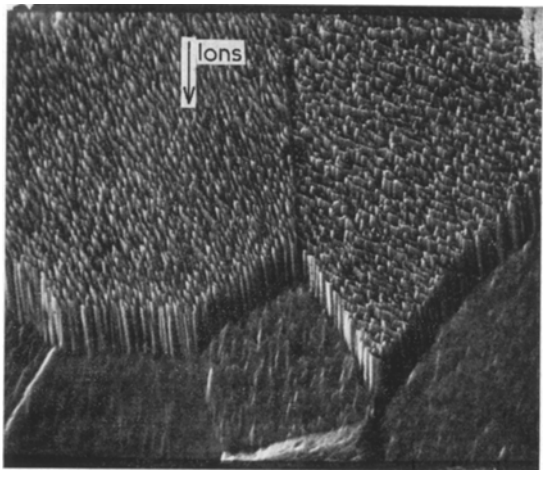


*Figure 5* Iron surface, bombarded with 20 keV $Ar^+$ ions at $\phi = 45°$ for 30 min ($t = 500°C$) × 3000.

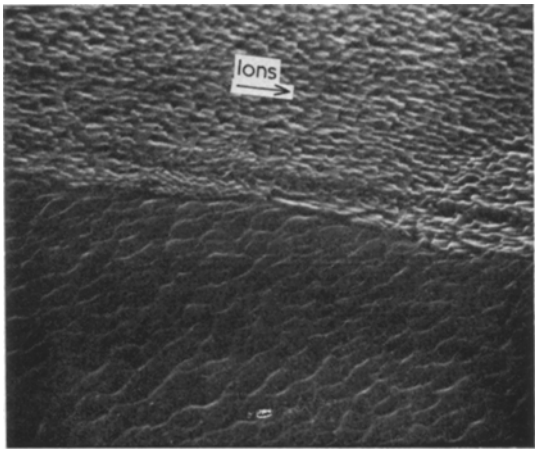


*Figure 4* Iron surface, bombarded with 20 keV $Ar^+$ ions at $\phi = 30°$ for 30 min ($t = 500°C$) × 3000.

at $t = 500°C$ for various incidence angles show that at this critical temperature the accelerated self-diffusion effects can begin to alter the ion eroded microtopography formed on some grains. A good example for $t = 500°C$, $\phi = 30°$ is seen in Fig. 4, where the ion erosion of the lower grain appears strongly modified as a result of thermal migration processes. However, some interesting effects of ion erosion can still occur in some localized areas for $t = 500°C$, $\phi = 45°$ (Fig. 5). The right-hand grain exhibits a common scale-shaped microrelief but on the left-hand grain, inclined at 45° to the surface normal and to the specimen surface, a large number of "needles" perpendicular to the grain micro-surface and oriented in the opposite direction to the ion beam, is observed. Two possible explanations can be proposed:

(a) Recently, Sigmund [7] has demonstrated that during the sputtering of a "ridge" pre-existing on surfaces or formed later during the sputtering, the surface regression speed varies from a maximum at the ridge base to a minimum value at the top of the ridge, being of an intermediary magnitude for ridge planes or a horizontal surface. Finally, this proposed mechanism leads to a theoretical prediction for the development of cones with very small apex angles (in fact real "needles") having an origin different from that of the conical spikes which have larger half angles and are usually formed during ion bombardment experiments [1, 15, 16];

(b) By using erosion slowness curves to predict ion eroded microtopography, Barber *et al.* [5] demonstrated that during erosion of some hemispherical protuberances existing on the sputtered surface, small-angle cones could be generated. These cones have a half angle $\alpha$ equal to $(\pi/2) - \theta$, where $\theta$ is the angle at which the sputtering yield is again equal to the value obtained with a normal incidence (evidently $\theta \approx 80°$ to 85° implying that $\alpha \approx 5°$ to 10°). It should also be noted that such non-eroded protuberances are also revealed on other micrographs corresponding to the same experimental conditions.

Another interesting aspect observed during ion erosion at $t = 500°C$ is related to the

formation of small pyramid-shaped growths in the regions adjacent to the bombardment area characteristic for the thermal etching of iron. However, the usual temperature for the growth of pyramids is 900 to 1000°C after a treatment of 30 min [14]. This decrease in threshold temperature for pyramid formation outside the bombarded area may be due to diffusion phenomena which are enhanced by ion bombardment, dislocation motion to the undamaged areas, and material transport by surface diffusion and sputtering.

For specimen temperatures exceeding the self-diffusion temperature $T_d$ (for iron $\approx$ 500°C), a surface flattening effect can clearly be observed for all incidence angles. An ion eroded microtopography formed due to the sputtering effects in association with a simultaneous thermal etching process, is presented in Fig. 6 for $t$ = 700°C and $\phi$ = 30°. At higher magnifications the fine details of etch line structure may be seen. Flattened structures are also observed at $t$=700°C, $\phi$=45° (Fig. 7) and 60° (Fig. 8) and a comparison of Figs. 2 and 3 with Fig. 5 shows the relevant points of the effect of increasing temperature on the characteristic microstructure for the same incidence angle, $\phi$ = 45°. An isolated "scale-shaped" microrelief due to ion etching at an incidence angle occurs at $t$ = 700°C, $\phi$ = 60° on a grain recently formed by recrystallization (Fig. 9).

An extensive pyramid formation is observed at the edge of the bombarded area at $t$ = 900°C, $\phi$ = 0° (Fig. 10). Two main points can be

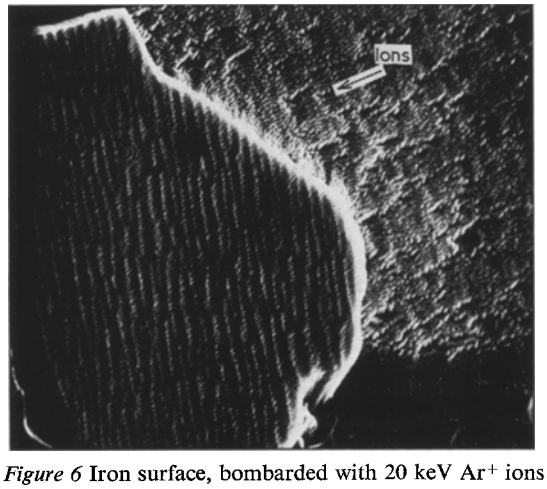


*Figure 6* Iron surface, bombarded with 20 keV $Ar^+$ ions at $\phi$ = 30° for 30 min ($t$ = 700°C) × 6000.

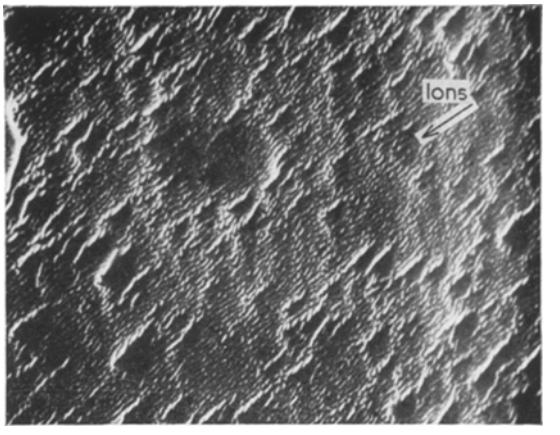


*Figure 7* Iron surface, bombarded with 20 keV $Ar^+$ ions at $\phi$ = 45° for 30 min ($t$ = 700°C) × 6000.

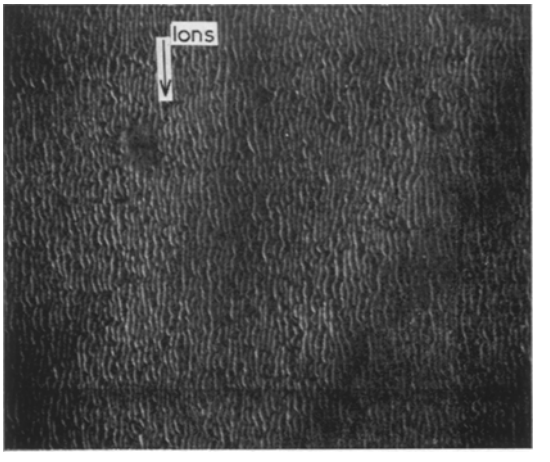


*Figure 8* Iron surface, bombarded with 20 keV $Ar^+$ ions at $\phi$ = 60° for 30 min ($t$ = 700°C) × 6000.

observed. (1) The pyramids are not formed on the ion bombarded area because of the conditions created by the simultaneous ion erosion. This disturbs the thermodynamic equilibrium which is necessary for the growth of pyramids at the points where the dislocations intersect the specimen surface and which can also induce a dislocation flow out of the area exposed to the ion beam. (2) The shape of many pyramids formed outside the bombarded area is strongly changed, compared to those originally formed (see Fig. 1a in [4]) thus suggesting a possible influence of diffusion effects, assisted by ion bombardment, allowing the migration of point and line defects (formed due to the displacement cascades induced in layers near the surface of

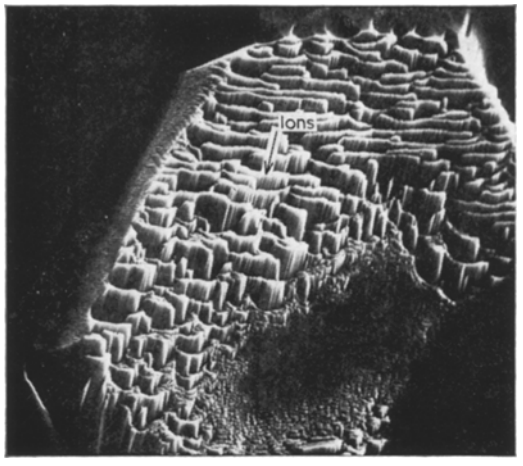


*Figure 9* Iron surface, bombarded with 20 keV $Ar^+$ ions at $\phi = 60°$ for 30 min ($t = 700°C$) × 3000.

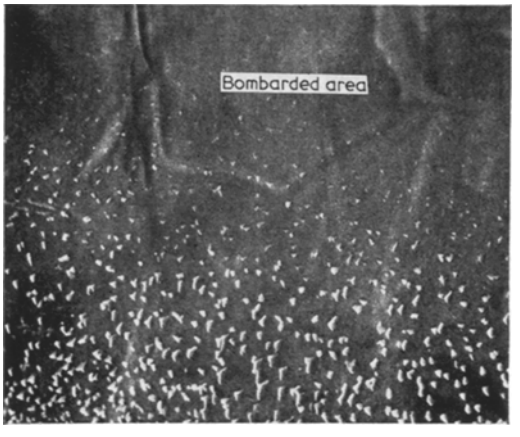


*Figure 10* Bombarded area boundary on iron surface, bombarded with 20 keV $Ar^+$ ions at $\phi = 0°$ for 30 min ($t = 900°C$) × 1000.

the irradiated area) to regions unaffected by ion irradiation (Fig. 11).

At $t = 900°C$, $\phi = 30°$, very shallow etch lines can only be observed at high magnifications. A TOPO-image (Fig. 12) allows a three-dimensional view of topographic profiles characteristic of these etch lines which seem very flattened in normal SEM images. A slight influence of directional ion erosion over the dominant thermal etching pattern is shown in Fig. 13 (for $t = 900°C$ and $\phi = 45°$). This shows a selective erosion of step surfaces formed by thermal etching. For $\phi > 60°$ these faint etch lines disappear as a consequence of small sputtering effects. Comparison of Figs. 3 and 13 reveals a predominance of ion etching at temperatures below $T_d$ (the role of specimen temperature being of secondary importance here for the development of surface microtopography) and a marked influence of thermal etching for specimen temperatures exceeding $T_d$, when overlapping of typical ion erosion features on the surface microtopography formed by thermal etching, is seen. During further heating of the specimen, the oriented erosion effects eventually flatten.

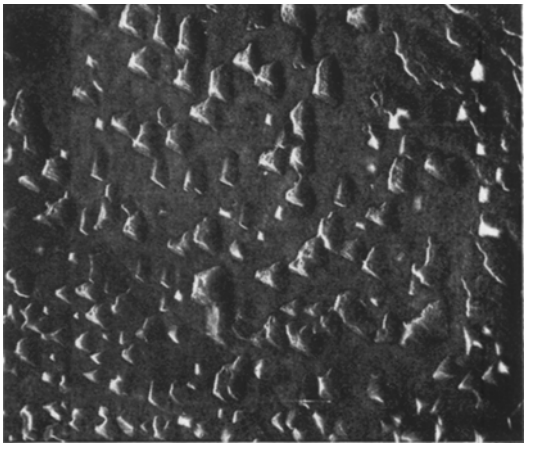

*Figure 11* Pyramids on unirradiated area of iron surface, bombarded with 20 keV $Ar^+$ ions at $\phi = 0°$ for 30 min ($t \parallel 900°C$) × 3000.

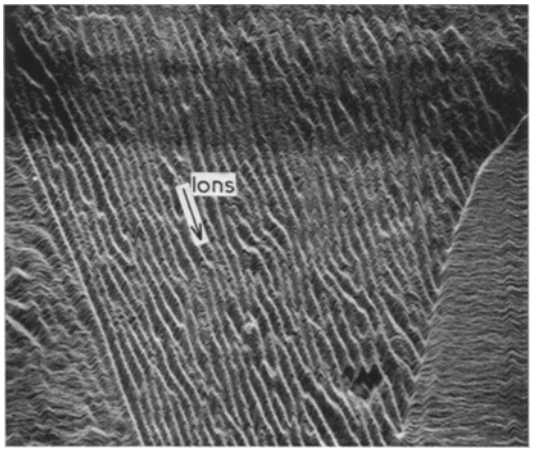


*Figure 12* TOPO-SEM micrograph of iron surface, bombarded with 20 keV $Ar^+$ ions at $\phi = 30°$ for 30 min ($t = 900°C$) × 6000.


*Figure 13* Iron surface, bombarded with 20 keV $Ar^+$ ions at $\phi = 45°$ for 30 min ($t = 900°C$) × 15 000.

The smoothing effect is generally increased at normal incidence or for $\phi > 60°$ when the values of sputtering yield, $S(\phi)$, are lower than those corresponding to $S_{max}(\phi \approx 60°)$ or $S(\phi = 30°)$ and $S(\phi = 45°)$. On the other hand, the penetration depth decreases with increasing $\phi$ so that the disturbed region moves nearer to the sample surface.

Between 300 and 1000 K, increasing temperature has been found to cause faster sputtering rates [17, 18], slower sputtering rates [18-20] but usually no change in the sputtering rate [18, 21-24] in mono- or polycrystalline metals. Unfortunately, experimental data for the temperature dependence of sputtering yield, $S$(atoms/ion), are very sparse and are for different metals and experimental conditions (ion beam nature, energy, flux, sample temperature). The absence of accurate measurements of angular dependence $S = S(\phi)$ performed at different temperatures for given values of the irradiation parameters, makes the discussion of the present SEM investigations difficult. In addition, the surface and volume diffusion effects, which are strongly dependent on specimen temperature, may have an important role as possible cancellation mechanisms for competing factors responsible for an increase (annealing of ion-bombardment damage, decrease in effective binding energy due to lattice vibration enhancement) or decrease (decreasing in the range of focused collision sequences) in sputtering yield with temperature.

The above results show that the microrelief formed during ion bombardment at high temperatures can be quite different from that expected and observed for low temperature irradiation. As the development of ion eroded microtopography is a surface phenomenon, various factors may be involved in the determination of the final surface structure:

(1) the amount of energy deposited by energetic particles (incident ions and recoil atoms) near the surface – the essential parameter of the surface erosion (sputtering) process;

(2) the surface and volume atomic migration:

– thermally induced diffusion and recrystallization

– surface migration assisted by ion bombardment (ion bombardment enhanced diffusion);

(3) the redeposition of the sputtered material;

(4) the effects of surface breakdown can sometimes play an important role depending on the electrical properties of the specimen and on the ion beam parameters.

## 4. Conclusions

(1) For specimen temperatures below the self-diffusion temperature $T_d$ (for iron $\approx 500°C$) ion erosion is the most influential effect, and the agglomeration and migration of defects and surface atoms do not influence the ion eroded microtopography.

(2) For specimen temperatures exceeding $T_d$, the surface topography is a result of ion erosion and thermal etching. A flattening process is observed and the selective ion etching features (etch lines, "scale-shaped" microrelief) appear to be formed on top of the thermal etching microstructure. This effect, due to the thermally-activated surface and volume diffusion, assisted by ion bombardment, is responsible for the constant values obtained for the sputtering yield $S$ of many metals at temperatures higher than 300°C.

(3) The pyramids commonly revealed by the thermal etching of iron at the dislocation ends intersecting the surface, do not appear within the ion bombarded area in spite of the fact that outside the area they occur at temperatures lower than normal for the usual thermal etching unassisted by ion bombardment. The influence of ion bombardment and surface radiation damage on the dynamic behaviour of dislocations and on the diffusion processes may be responsible for the modification of oriented crystal growth.

## Acknowledgements

We would like to thank Professors P. Sigmund

and G. Carter for valuable discussions, about this work. Thanks are also due to Mrs E. Reissler and Mr A. Reissler for their help with the experimental work.

## References

1. A. D. G. STEWART and M. W. THOMPSON, *J. Mater. Sci.* **4** (1969) 56.
2. W. HAUFFE, *Phys. Stat. Sol. (a)* **4** (1971) 111.
3. I. TEODORESCU, *Rev. Roum. Phys.* **12** (1967) 305.
4. I. A. TEODORESCU and F. VASILIU, *Rad. Effects* **15** (1972) 101.
5. D. J. BARBER, F. C. FRANK, M. MOSS, J. W. STEEDS and I. S. T. TSONG, *J. Mater. Sci.* **8** (1973) 1030.
6. G. CARTER, J. S. COLLIGON and M. J. NOBES, *ibid* **8** (1973) 1473.
7. P. SIGMUND, *ibid* **8** (1973) 1545.
8. A. R. BAYLY, *ibid* **7** (1972) 404.
9. N. HERMANNE and A. ART, *Rad. Effects* **5** (1970) 203.
10. R. S. NELSON and D. J. MAZEY, *ibid* **18** (1973) 127.
11. N. HERMANNE, *ibid* **19** (1973) 161.
12. G. V. SPIVAK, I. N. PRILEZHAEVA and O. I. SAVOCHKINA, *Dokl. Acad. Nauk. SSR* **88** (1953) 511.
13. M. T. ROBINSON and A. L. SOUTHERN, *J. Appl. Phys.* **39** (1968) 3470.
14. I. A. TEODORESCU and I. ZBEREA, *Rev. Roum. Phys.* **12** (1967) 721.
15. I. H. WILSON and M. W. KIDD, *J. Mater. Sci.* **6** (1971) 56.
16. I. H. WILSON, *Rad. Effects* **18** (1973) 95.
17. J. M. FLUIT, C. SNOECK and J. KISTEMAKER, *Physica* **30** (1964) 144.
18. C. E. CARLSON, G. D. MAGNUSON, A. COMEAUX and P. MAHADEVAN, *Phys. Rev.* **138** (1965) 759.
19. O. ALMEN and G. BRUCE, *Nucl. Instr. Methods* **11** (1961) 257.
20. T. V. SNOUSE and M. BADER, *Trans. Sec. Int. Vac. Congr.* **1** (1962) 271.
21. J. M. FLUIT, "Le Bomb. ionique", Ed. CNRS (1962) p. 119.
22. J. B. SANDERS and J. M. FLUIT, *Physica* **30** (1964) 129.
23. M. KOEDAM, *Phillips Res. Rep.* **16** (1961) 101, 266.
24. R. S. BHATTACHARYA, D. K. MUKHERJEE and S. B. KARMOHAPATRO, *Nucl. Instr. Methods* **99** (1972) 509.

Received 17 July and accepted 24 July 1974.